Materials Science & Engineering A 556 (2012) 671–677

Contents lists available at SciVerse ScienceDirect

Materials Science & Engineering A

journal homepage: www.elsevier.com/locate/msea

Influence of texture on superplastic behavior of friction stir processed ZK60 magnesium alloy

Q. Yang, A.H. Feng, B.L. Xiao, Z.Y. Ma*

Shenyang National Laboratory for Materials Science, Institute of Metal Research, Chinese Academy of Sciences, 72 Wenhua Road, Shenyang 110016, China

ARTICLE INFO

Article history:
Received 16 May 2012
Received in revised form
3 July 2012
Accepted 10 July 2012
Available online 20 July 2012

Keywords:
Superplasticity
Magnesium alloys
Friction stir processing
Texture

ABSTRACT

Commercial ZK60 extruded plate was subjected to friction stir processing (FSP). A fine-grained structure 2.9 μm in grain size with uniformly distributed fine second-phase particles and predominant high-angle grain boundaries of 97% was obtained. A strong basal fiber texture with the (0002) planes roughly surrounding the tool pin surface was developed in the FSP ZK60 alloy. The FSP ZK60 alloy exhibited superplastic behavior at 225–325 °C in both the transverse direction (TD) and longitudinal direction (LD), with the superplastic elongation in the LD being higher than that in the TD. A maximum elongation of 1390% was obtained at 300 °C and $3 \times 10^{-4}\ s^{-1}$ in the LD. The existence of texture was found to influence the superplastic flow stress and plasticity. The texture had a minor influence on the flow stress, due to the texture weakening during superplastic deformation. However, the anisotropy of plasticity existed at all temperatures and strain rates, as a result of the activation of different slip systems in different tensile directions.

1. Introduction

Magnesium alloys have recently attracted significant interest due to their excellent specific strength, which makes them promising candidates for structural materials. The main limitation to the wide application of magnesium alloys is their poor formability at room temperature. Superplastic forming is an effective method of fabricating magnesium alloys into complex shapes.

It is generally accepted that fine grains with a grain size of less than 10 μm are needed to obtain superplasticity [1]. Therefore, studies on the superplastic deformation of magnesium alloys have mainly been focused on optimizing the microstructure via various plastic deformation methods, such as equal channel angular pressing (ECAP) [2–4], hot rolling [5], extrusion [6], friction stir processing (FSP) [7,8], and differential speed rolling (DSR) [9]. However, as commonly observed in hexagonal close-packed metals, texture was often developed and was proved to influence the mechanical properties of magnesium alloys at both room and high temperatures [10]. Until now, only limited studies of the influence of texture on superplasticity are available [11–15]. These investigations indicate that, although texture weakening during superplastic deformation due to the occurrence of grain boundary sliding (GBS) is commonly observed [12–15], the influence of texture on the superplasticity of magnesium alloys is still in dispute.

A study of AM60 magnesium alloy suggested that texture had no detectable effect on the superplastic behavior [15], while studies on MA15 and AZ31 magnesium alloys indicated that texture influenced both the flow stress and superplastic elongation [11,16]. However, variations in grain shape, grain size, grain size distribution and the grain boundary structure could also influence the superplastic behavior, and these may cause misleading results when considering the influence of texture [17–19]. Therefore, these factors should be fixed when evaluating the influence of texture on superplasticity. One promising method for overcoming such problems is to evaluate the superplastic behavior on the same sample which has uniform and equiaxed grains but different texture components when tested in different directions.

FSP, a development based on the friction stir welding (FSW) technique, is a promising method of producing this kind of microstructure. Previous studies revealed that fine and equiaxed grains could be produced in the magnesium alloys by FSP, and as a result of complex deformation during FSP, varied texture distributions were formed in the FSP magnesium alloys [7,20–23]. In addition, several FSP magnesium alloys, such as AZ91, AM60B, and Mg–Zn–Y–Zr, were reported to exhibit superior superplasticity due to the refined microstructure [7,20,21].

In this study, an attempt was made to prepare the fine-grained ZK60 magnesium alloy with uniform and equiaxed grains but different texture components in different directions by FSP under

* Corresponding author. Tel./fax: +86 24 83978908.
E-mail address: zyma@imr.ac.cn (Z.Y. Ma).

0921-5093/$ - see front matter © 2012 Elsevier B.V. All rights reserved.
http://dx.doi.org/10.1016/j.msea.2012.07.046

an accelerated cooling condition, and the superplastic deformation behavior of the FSP ZK60 alloy was investigated under various testing temperatures and strain rates. The aim is to understand the influence of texture on the superplastic properties of the fine-grained magnesium alloy.

2. Experimental

ZK60 extruded plate of 6 mm thickness was subjected to FSP at a rotation rate of 1000 rpm and a traverse speed of 100 mm/min. A tool with a concave shoulder 12 mm in diameter, a threaded cylindrical pin 4 mm in diameter, and 4 mm in length was used. To accelerate the cooling of the FSP sample, a copper backplane was used. Principle directions of the FSP sample were marked as the LD (longitudinal direction, along the FSP direction), the TD (transverse direction, transverse to the FSP direction), and the ND (normal direction, normal to the plate surface).

Mini tensile specimens (2.5 mm gage length, 1.4 mm gage width, and 1.0 mm gage thickness) were machined along both the TD and LD with the gage being completely in the stir zone (SZ). The specimens were subsequently ground and polished to a final thickness of 0.8 mm. Tensile tests were carried out using an Instron 5848 microtester. For the room temperature tensile test, the specimens were tested at a constant initial strain rate of $1\times10^{-3}\,s^{-1}$. For the superplastic test, each specimen was fastened in the tensile testing apparatus when the furnace was heated to the selected testing temperature and then held at that temperature for 15 min to establish thermal equilibrium prior to the tensile test.

Microstructural characterization of both the extruded and the FSP samples was performed by optical microscopy (OM) and scanning electron microscopy (SEM, HITACHI S-3400N). Specimens for OM and SEM were prepared by mechanical polishing and etching using a solution consisting of 4.2 g picric acid + 10 ml acetic acid + 70 ml ethanol + 10 ml water. Electron backscatter diffraction (EBSD) orientation maps were obtained using a ZEISS SUPRA 35. Both the non-deformed and deformed samples for EBSD were prepared by electrochemical polishing with commercial AC2 electrolyte, at 25 V and 20 °C. The EBSD data were collected from the SZ center for the non-deformed sample and near the fracture tip for the deformed sample, respectively.

3. Results

Fig. 1 shows the microstructure of the extruded and FSP ZK60 alloy samples. The microstructure of the extruded ZK60 alloy exhibited the typical banded structure with large elongated grains and fine recrystallized grains (Fig. 1a), and the SEM image revealed the stripe-like distribution of the second-phase particles (Fig. 1c). By comparison, a uniform fine-grained structure 2.9 μm in grain size with uniformly distributed fine particles was observed in the FSP sample (Fig. 1b and d). Such fine-grained microstructure was the same in different cross-sections of the FSP sample.

Fig. 2a shows the microstructure of the FSP ZK60 alloy obtained by EBSD mapping. High-angle grain boundaries (HAGBs, grain boundary misorientations $\geq 15^{\circ}$) and low-angle grain boundaries (LAGBs, grain boundary misorientations $<15^{\circ}$) are shown by black and white lines, respectively. The microstructure was characterized by equiaxed grains with predominant HAGBs, and the fraction of the HAGBs was determined to be 97% (Fig. 2b). Fig. 2c shows the pole figures in the SZ center of the FSP ZK60 alloy. A strong and simple basal fiber texture was present, with the basal plane normal being parallel to the LD.

Fig. 3 presents the room temperature tensile curves of the FSP ZK60 alloy in the TD and LD. The results from both tensile tests are summarized in Table 1. A strong anisotropic behavior with much higher yield strength and significantly lower ductility in the TD than in the LD is clearly observed, though the ultimate tensile strengths in both directions were almost the same.

Fig. 4 shows the variations of elongation of the FSP ZK60 alloy with the initial strain rate in both the TD and LD at different temperatures. Superplasticity was observed in both directions. In the LD, as shown in Fig. 4a, when increasing temperature, the tensile elongation and the optimum strain rate increased initially and then decreased; the largest elongation of 1180% was obtained

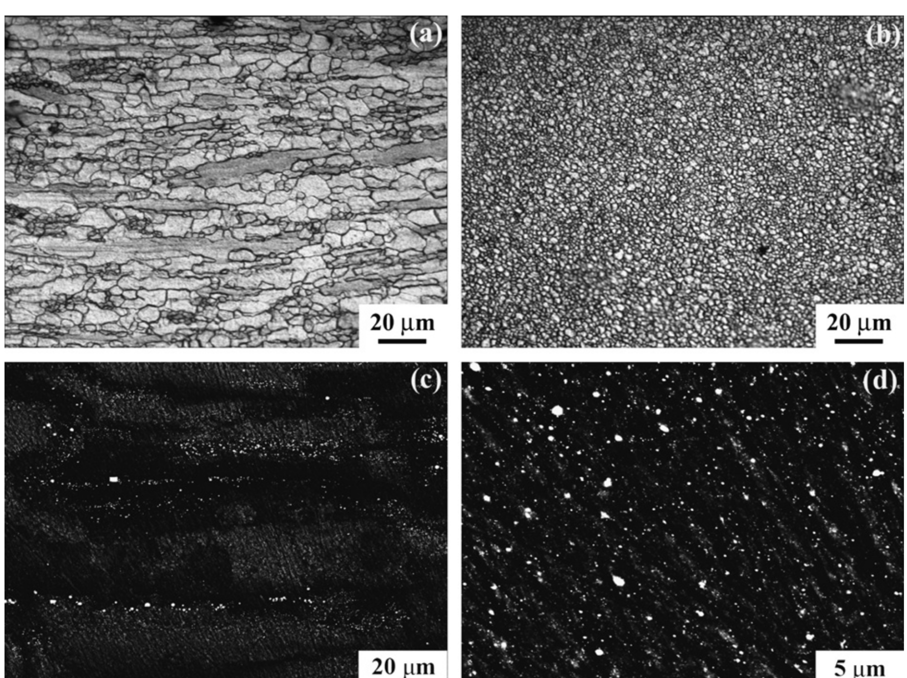

Fig. 1. OM and SEM micrographs showing the microstructure of ZK60 alloy: (a) and (c) extruded sample; (b) and (d) FSP sample.

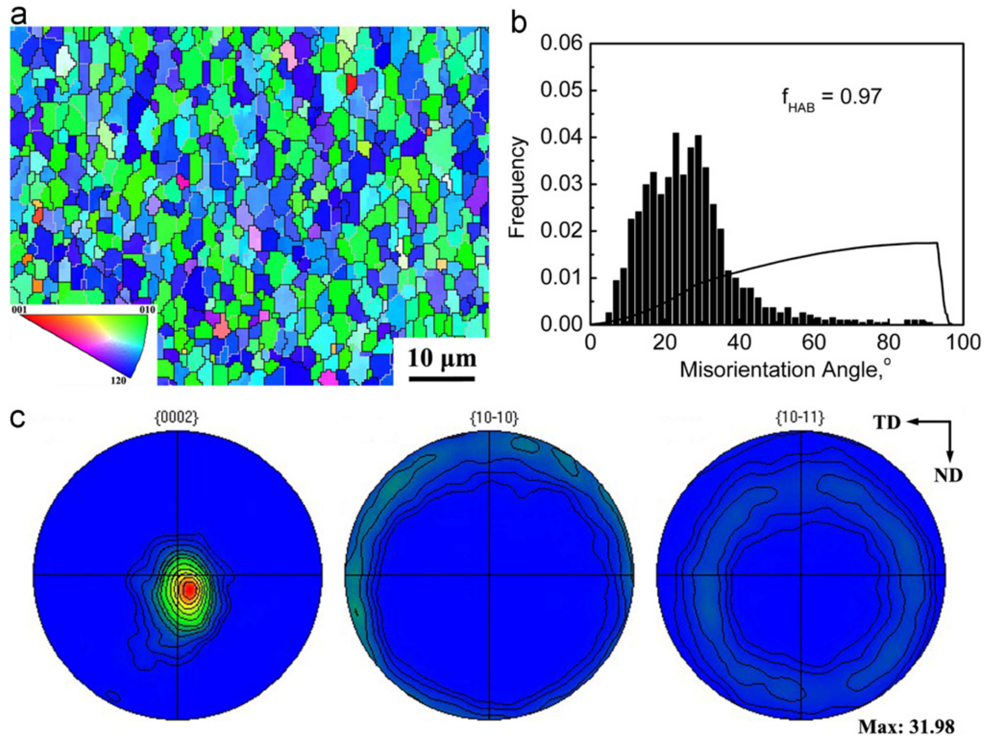

Fig. 2. Microstructure of FSP ZK60 alloy: (a) EBSD map, (b) boundary misorientation angle distribution, and (c) pole figures.

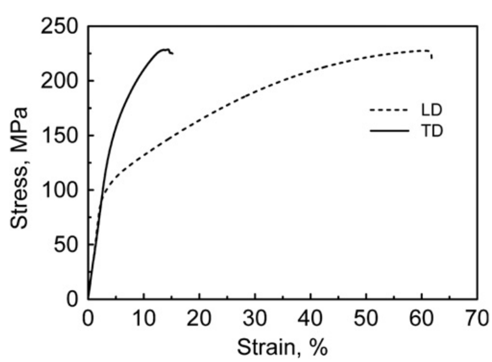

Fig. 3. Room temperature stress–strain curves of FSP ZK60 alloy.

Table 1
Tensile properties of FSP ZK60 alloy at room temperature.

Direction	YS (MPa)	UTS (MPa)	El. (%)
TD	130	229	8.7
LD	92	228	55.8

at 275 °C and a strain rate of $3 \times 10^{-4}\,s^{-1}$. Compared with the TD specimens, enhanced elongation was observed in the LD specimens in the temperature range from 250 °C to 300 °C (Fig. 4b). The optimum superplastic temperature shifted from 270 °C in the TD to 300 °C in the LD, with the maximum elongation of 1390% being obtained at a strain rate of $3 \times 10^{-4}\,s^{-1}$.

Fig. 5 shows the variation of flow stress with the initial strain rate for the FSP ZK60 alloy in both the TD and LD. A minor difference in flow stress between the TD and LD samples was observed. A strain rate sensitivity m of ~0.5 was observed in both the TD and LD specimens in the investigated temperature range.

Fig. 6 compares the superplastic elongation of the TD and LD specimens as functions of temperature and strain rate for the FSP ZK60 alloy. Distinct plastic anisotropy was observed. As shown in Fig. 6a, at a constant initial strain rate of $3 \times 10^{-4}\,s^{-1}$, the elongation in the LD was higher than that in the TD in the investigated temperature range. At 300 °C, the superplastic elongation in the LD was higher than in the TD at all tested strain rates (Fig. 6b).

Fig. 7 shows the flow stress of the TD and LD specimens as functions of the temperature and strain rate for the FSP ZK60 alloy. As shown in Fig. 7a, at a constant strain rate of $3 \times 10^{-4}\,s^{-1}$, the flow stress decreased as the temperature increased. Flow stress anisotropy was observed at 225 °C, with higher flow stress in the TD than in the LD. However, this flow stress anisotropy nearly disappeared above 250 °C. At a constant temperature of 300 °C, the flow stress decreased with decreasing strain rate (Fig. 7b). Distinct flow stress anisotropy was observed at a high strain rate of $1 \times 10^{-2}\,s^{-1}$. The flow stress anisotropy decreased as the strain rate decreased and disappeared at strain rates below $3 \times 10^{-4}\,s^{-1}$.

Fig. 8 shows the true stress—true strain curves of the FSP ZK60 alloy in the TD and LD at 250 °C and $3 \times 10^{-4}\,s^{-1}$. The superplastic flow curves exhibited a strain softening behavior in both directions.

Fig. 9 shows the typical surface morphology of the FSP ZK60 alloy deformed at 250 °C and $3 \times 10^{-4}\,s^{-1}$ in both the TD and LD. Distinct evidence of GBS was observed in both the TD and LD specimens. Similar morphologies were also observed under other deformation conditions.

Fig. 10 shows the EBSD maps of the FSP ZK60 alloy after superplastic deformation in the TD and LD at 250 °C and $3 \times 10^{-4}\,s^{-1}$. Grain growth and grain elongation occurred during deformation in both directions. The grain size parallel and perpendicular to the tensile direction was estimated to be 7.2 μm and 4.9 μm for the TD tension, and 8.7 μm and 4.2 μm for the LD tension, respectively.

Fig. 11 shows the texture distributions of the FSP ZK60 alloy after superplastic deformation in the TD and LD at 250 °C and $3 \times 10^{-4}\,s^{-1}$. Compared with the initial texture, distinct texture weakening was observed in both directions. The texture distributions

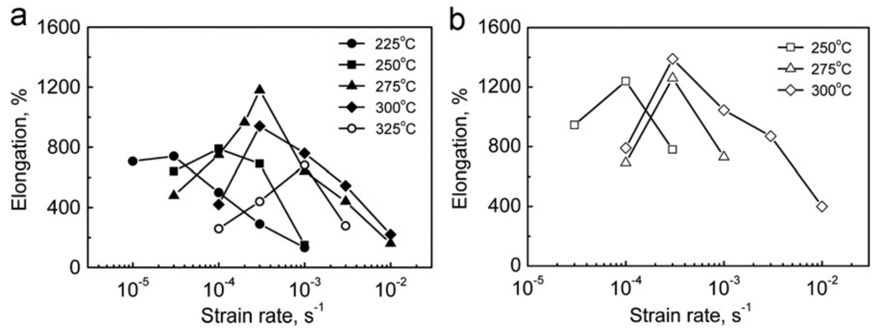

Fig. 4. Variation of elongation with initial strain rate for FSP ZK60 alloy tested in (a) TD and (b) LD.

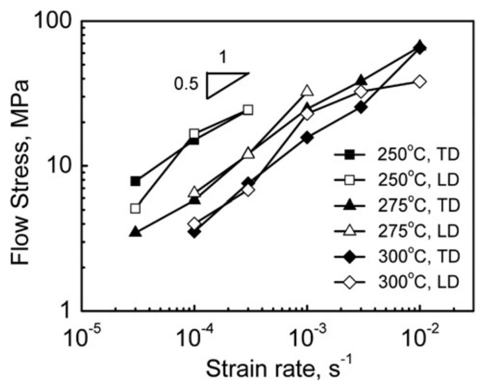

Fig. 5. Variation of flow stress with initial strain rate for FSP ZK60 alloy.

after superplastic deformation were quite different in the TD and LD. A spreading out of basal texture was observed in the TD tension (Fig. 11a). However, the rotation and splitting of the basal pole was evident in the LD tension (Fig. 11b).

4. Discussion

The microstructure of the FSP ZK60 alloy was characterized by fine and equiaxed grains. Furthermore, fine second-phase particles were distributed uniformly throughout the magnesium matrix. Such a microstructure is typical of FSW/FSP alloys as a result of intense plastic deformation and dynamic recrystallization [8]. The high percentage of HAGBs in the FSP sample also suggested the occurrence of dynamic recrystallization during FSP. By using the copper backplane to accelerate the cooling, the growth of the recrystallized grains was significantly suppressed. Therefore, the grain size in the FSP ZK60 was finer than that in the reported FSW/FSP magnesium alloys [7,20].

It is documented that in the SZ of FSW/FSP alloys, the texture distribution is affected by both the tool shoulder and the rotating pin [23–25]. The tool shoulder can generate compressive stress in regions about 0.5 mm from the upper surface and cause a complex texture distribution in these regions [22,24]. However, the rotating pin can affect all regions in the SZ and generate a shear deformation with the (0002) planes aligning with an ellipsoidal surface surrounding the rotating pin in magnesium alloys [22,26]. Such a pin-affected region often presents an elliptical shape. In the FSP ZK60 alloy, a simple and strong basal fiber texture was observed in the center of the SZ (Fig. 2c). Besides, the SZ exhibited an elliptical shape (not shown), indicating that the SZ was generated by the rotating pin. Therefore, the texture component in the SZ was the basal fiber texture, with the (0002) planes roughly surrounding the tool pin surface. During tensile testing, the *c* axis was roughly perpendicular to the tensile direction in the TD and parallel to the tensile direction in the LD.

As seen from Fig. 3 and Table 1, the room-temperature tensile properties were different in the TD and LD, higher elongation and lower yield strength were observed in the LD. It is suggested that during tension along the *c* axis, $\left\{10\bar{1}2\right\}$ twining could readily occur in the early stage of deformation and result in a low yield stress [27,28]. However, in the FSP ZK60 alloy, twinning could hardly occur in the LD tension, because the flow curve in the LD tension is convex rather than the "s" shape that is a signature of twinning [29]. In addition, the fine grains and fine particles could inhibit twinning. Another explanation for the low yield stress in tension along the *c* axis is the better chance for the activation of slip systems than that in tension perpendicular to the *c* axis [30]. Therefore, the anisotropy of yield strength and elongation in the FSP ZK60 alloy is more likely to be caused by the activation of different slip systems rather than by twinning.

For the FSP ZK60 alloy, superplasticity was observed in both the TD and LD in the investigated temperature range of 225–325 °C (Fig. 4); a high elongation of above 1000% was obtained in both directions at low strain rates. This was attributed to the fine grains and dispersed second-phase particles after FSP, as shown in Fig. 1. The *m* value of ~0.5 and the distinct evidence of GBS on the surfaces of deformed specimens suggest that the main deformation mechanism is GBS in both directions. Such low strain rate superplasticity was also observed in previous studies of ZK60 alloy, produced by other plastic deformation methods [4,31].

Although superplasticity was observed in both directions, a difference in superplastic properties existed between the TD and LD specimens (Figs. 6 and 7). As shown in Figs. 5 and 7, the flow stress anisotropy in the TD and LD was minor at temperatures above 225 °C and strain rates lower than $1\times10^{-3}\,s^{-1}$. However, higher elongation was observed in the LD than in the TD in the investigated temperature and strain rate ranges. In addition, higher optimum superplastic temperature was observed in the LD. These differences cannot result from the difference in the microstructure, because the equiaxed grains with dispersed fine particles and the grain boundary structure were the same in both directions. In addition, the similar superplastic flow curves in the TD and LD indicated that similar microstructure change occurred during superplastic deformation in both directions. Therefore, the difference of superplastic properties in the TD and LD was caused by the texture.

Previous studies suggested that during superplastic deformation, GBS was expected to rotate the grains randomly and cause overall weakening of the texture [12–15]. Besides, the temperature and strain rate could influence this texture effect; higher temperature and lower strain rate resulted in accelerated texture weakening [12,32]. As a result, the anisotropy of flow stress decreased during superplastic deformation and further decreased at higher temperatures or lower strain rates.

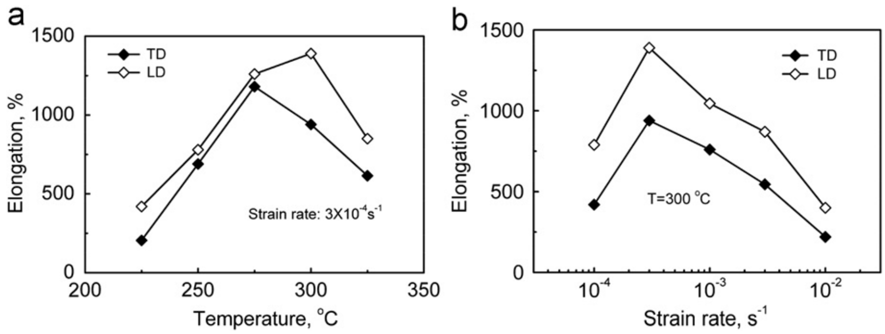

Fig. 6. Variations of elongation with (a) temperature and (b) initial strain rate for FSP ZK60 alloy in TD and LD.

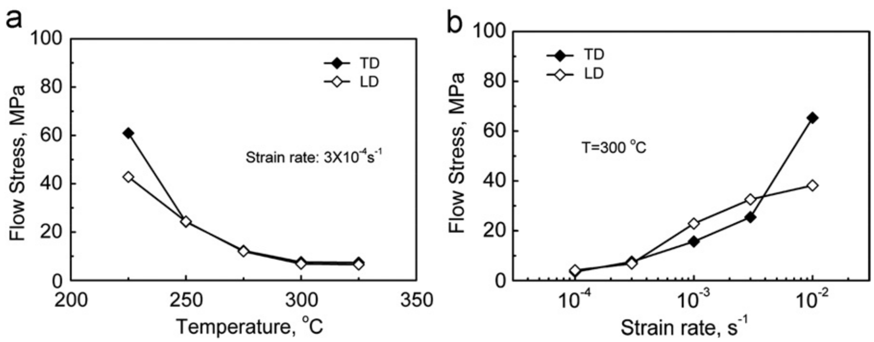

Fig. 7. Variations of flow stress with (a) temperature and (b) initial strain rate for FSP ZK60 alloy in TD and LD.

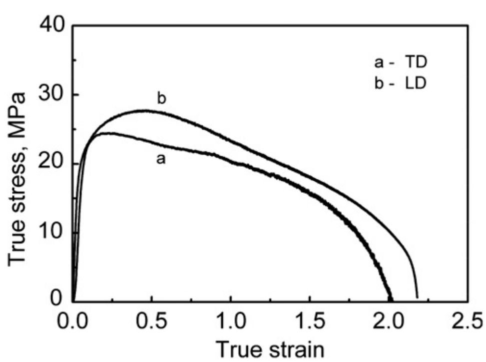

Fig. 8. True stress–true strain curves for FSP ZK60 alloy superplastically deformed to failure at 250 °C and 3×10^{-4} s^{-1} in TD and LD.

For the FSP ZK60 alloy, the decrease of flow stress anisotropy at above 225 °C was also a result of texture weakening, because the occurrence of GBS was evident on the surfaces of deformed specimens in both directions, and the texture intensity after deformation was significantly weakened (Figs. 9 and 11). Note that the flow stress anisotropy persisted at 225 °C but decreased above 250 °C. The easy occurrence of non-basal slip at temperatures above 225 °C and the decrease of critical resolved shear stress (CRSS) of the non-basal slip with increasing temperature could account for this difference in the flow stress anisotropy. On the other hand, the flow stress anisotropy decreased with decreasing strain rate at 300 °C (Fig. 7b). This was the result of further texture weakening due to a longer time in lower strain rate tests.

Although the flow stress anisotropy in the FSP ZK60 alloy was reduced during superplastic deformation, the plastic anisotropy remained at all testing temperatures and strain rates (Figs. 4 and 6). The grain elongation after superplastic deformation indicated that grain matrix slip deformation operated during deformation [14]. Furthermore, the texture evolved differently when tested in different directions, as shown in Fig. 11. Therefore, the plastic anisotropy could be explained by the difference of texture evolution. Previous investigations indicated that, although the overall texture was weakened during superplastic deformation, several texture components were retained after deformation due to the dislocation motion [12,15,33].

For the rolled or extruded magnesium alloys with a basal fiber texture, when the tensile direction is perpendicular to the *c* axis at elevated temperatures, the prismatic $<a>$ slip occurred preferentially and generated rotations around the *c* axis, without reorientation of the latter [34]. As a result, the basal texture remained with a rotation of the *c* axis towards the tensile direction [15,35]. However, when both GBS and prismatic $<a>$ slip occurred, the GBS would suppress the preferential rotation of grains and cause a spreading out of the basal texture [15]. When the loading direction is parallel to the *c* axis, only pyramidal $<c+a>$ slip and twinning could accommodate the deformation [36]. The occurrence of $<c+a>$ slip could cause rotation and splitting of the *c* axis, while twinning reorients the *c* axis [34].

In the FSP ZK60 alloy, the spreading out of the basal texture after superplastic deformation in the TD indicated the predominance of prismatic $<a>$ slip during superplastic deformation (Fig. 11a). The rotation and splitting of the basal pole after superplastic deformation in the LD was indicative of the occurrence of pyramidal $<a+c>$ slip, as reported by Agnew et al. [34]. Therefore, it is concluded that the activation of $<a+c>$ slip in the LD could result in higher superplasticity than the activation of prismatic $<a>$ slip in the TD did. The activation of these non-basal slip systems was promoted as the superplastic temperature increased. Consequently, higher elongation was observed in the LD at all temperatures and strain rates.

The influence of texture on the superplastic properties was studied previously. Kaibyshev et al. [11] observed the anisotropy of flow stress and plastic behavior of an upset MA15 magnesium alloy even at 500 °C. By fixing the grain size and grain size distribution, Valle and Ruano [14] found that the flow stress in

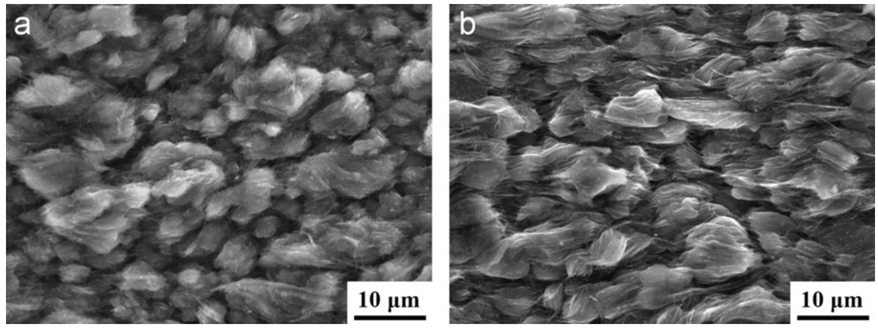

Fig. 9. Surface morphologies of FSP ZK60 alloy superplastically deformed to failure at 250 °C and $3\times10^{-4}\,s^{-1}$ in (a) TD and (b) LD (tensile axis is horizontal).

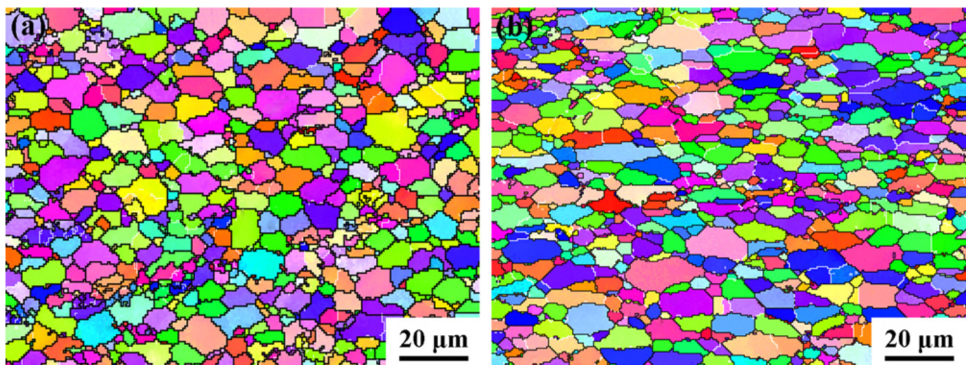

Fig. 10. EBSD maps of FSP ZK60 alloy after superplastic deformation at 250 °C and $3\times10^{-4}\,s^{-1}$ in (a) TD and (b) LD (tensile axis is horizontal).

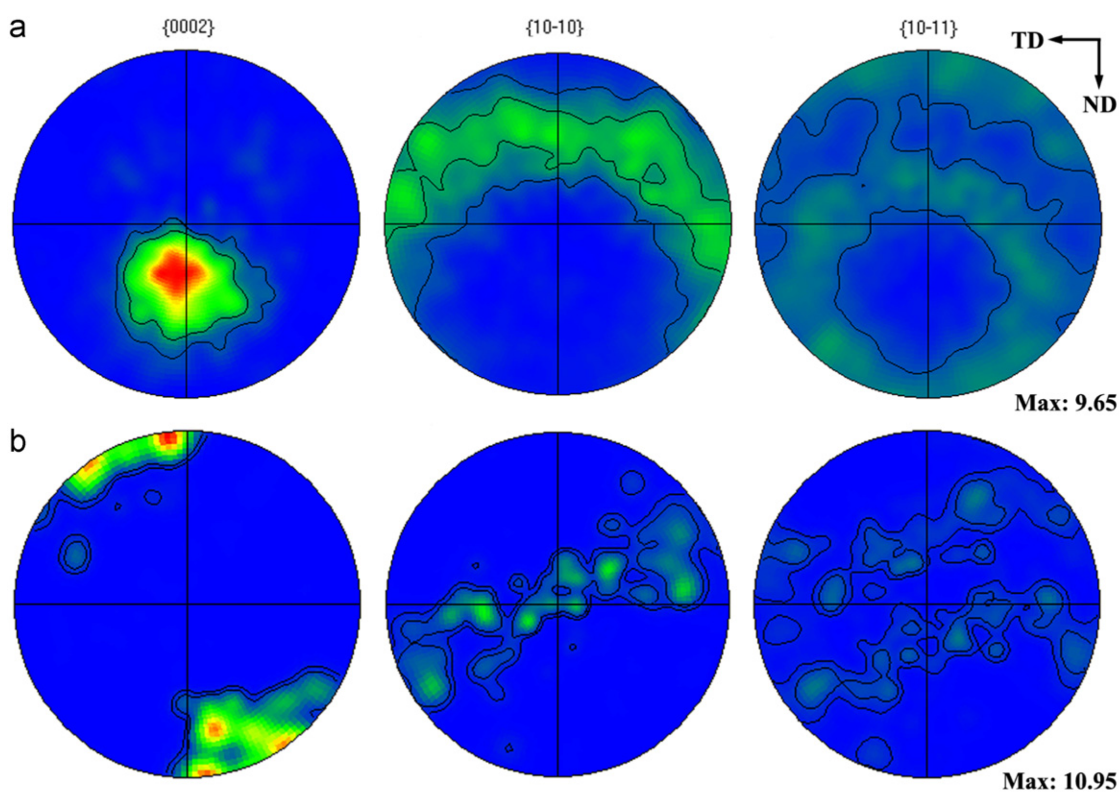

Fig. 11. Pole figures of FSP ZK60 alloy after superplastic deformation at 250 °C and $3\times10^{-4}\,s^{-1}$ in (a) TD and (b) LD.

the cast, ECAP, and rolled AM60 alloy were the same. The present work on FSP ZK60 alloy revealed that, the texture had a minor influence on the flow stress anisotropy, while an obvious plastic anisotropy was observed.

These differences could be attributed to the difference in texture weakening speed, and are influenced by the following three factors. Firstly, higher contribution of GBS could rotate the grains more randomly and thus accelerate the texture weakening.

Consequently, the flow stress anisotropy could be further reduced. It is reported that fine grains and a high percentage of HAGBs are beneficial to GBS [17]. For the upset MA15 alloy studied in [11], GBS might not have occurred sufficiently due to the relatively large grains (9 μm), which could be verified by the low *m* values in the study. As a result, the flow stress anisotropy remained at all testing temperatures. In this study, the fine grains and high percentage of HAGBs could facilitate the occurrence of GBS and then weakened the texture significantly. Consequently, there was a rapid decrease of flow stress anisotropy in the FSP ZK60 alloy.

Secondly, besides the GBS, the initial texture could also influence the texture evolution during superplastic deformation. Watanabe et al. [37] observed that the speed of texture weakening of the extruded AZ91 alloy in a sheet form was higher than that in a rod form. Therefore, although the initial texture was different in the cast, ECAP, and rolled AM60 alloy in [14], the texture weakening speed might also be different in these samples, hence the same flow stress was observed.

Thirdly, as discussed above, the angle between the tensile direction and the *c* axis could activate different slip systems. This, in turn, results in a difference in the texture weakening speed. Because of this, the plastic anisotropy of the upset MA15 alloy [11] and the FSP ZK60 alloy was preserved. Detailed studies are needed to understand the factors that influence the texture weakening speed during superplastic deformation, the relationship between texture and GBS, and the combined influence of texture and GBS on superplasticity.

5. Conclusions

1. A fine-grained ZK60 alloy, prepared by FSP, exhibited an equiaxed fine-grained structure with a grain size of 2.9 μm, a high percentage of HAGBs, and a strong basal fiber texture with the basal planes surrounding the tool pin surface.
2. The FSP ZK60 alloy exhibited superplasticity at 225–325 °C in both the TD and LD, with superplastic elongation in the LD being higher than those in the TD. The maximum superplasticity of 1390% was observed at 300 °C and $3 \times 10^{-4}\,s^{-1}$ in the LD.
3. The texture in the FSP ZK60 alloy had a minor influence on the flow stress anisotropy at above 250 °C, due to the texture weakening during superplastic deformation.
4. Higher superplasticity in the LD than in the TD at all temperatures and strain rates was attributed to the activation of different slip systems in different directions.

Acknowledgments

This work was supported by (a) the National Natural Science Foundation of China under Grant no. 50901075, (b) the National Basic Research Program of China under Grant no. 2011CB606301 and (c) the National Outstanding Young Scientist Foundation of China under Grant no. 50525103.

References

[1] O.D. Sherby, J. Wadsworth, Prog. Mater. Sci. 33 (1989) 169–221.
[2] R.B. Figueiredo, T.G. Langdon, Adv. Eng. Mater. 10 (2008) 37–40.
[3] R.B. Figueiredoa, T.G. Langdon, Scripta Mater. 61 (2009) 84–87.
[4] H. Watanabe, T. Mukai, K. Ishikawa, K. Higashi, Scripta Mater. 46 (2002) 851–856.
[5] Y. Kim, D. Bae, Mater. Trans. 45 (2004) 3298–3303.
[6] S.S. Park, B.S. You, Scripta Mater. 65 (2011) 202–205.
[7] Q. Yang, B.L. Xiao, Z.Y. Ma, R.S. Chen, Scripta Mater. 65 (2011) 335–338.
[8] R.S. Mishra, Z.Y. Ma, Mater. Sci. Eng. R 50 (2005) 1–78.
[9] W.J. Kim, B.H. Lee, J.B. Lee, M.J. Lee, Y.B. Park, Scripta Mater. 63 (2010) 772–775.
[10] P. Mehrotra, T.M. Lillo, S.R. Agnew, Scripta Mater. 55 (2006) 855–858.
[11] O.A. Kaibyshev, I.V. Kazachkov, N.G. Zaripov, J. Mater. Sci. 23 (1988) 4369–4374.
[12] K.N. Melton, J.W. Edington, J.S. Kallend, G.P. Cutler, Acta Metall. 22 (1974) 165–170.
[13] H. Watanabe, A. Takara, H. Somekawa, T. Mukai, K. Higashi, Scripta Mater. 52 (2005) 449–454.
[14] J.A.d. Valle, O.A. Ruano, Acta Mater. 55 (2007) 455–466.
[15] R. Panicker, A.H. Chokshi, R.K. Mishra, R. Verma, P.E. Krajewski, Acta Mater. 57 (2009) 3683–3693.
[16] H.K. Lin, J.C. Huang, T.G. Langdon, Mater. Sci. Eng. A 402 (2005) 250–257.
[17] Z.Y. Ma, R.S. Mishra, M.W. Mahoney, R. Grimes, Metall. Mater. Trans. A 36A (2005) 1447–1457.
[18] D.S. McDarmaid, A.W. Bowen, P.G. Partridge, J. Mater. Sci. 20 (1985) 1976–1984.
[19] Z.Y. Ma, R.S. Mishra, M.W. Mahoney, Acta Mater. 50 (2002) 4419–4430.
[20] P. Cavaliere, P.P.D. Marco, J. Mater. Process. Technol. 184 (2007) 77–83.
[21] P. Cavaliere, P.P.D. Marco, Mater. Sci. Eng. A 462 (2007) 393–397.
[22] S.H.C. Park, Y.S. Sato, H. Kokawa, Metall. Mater. Trans. A 34A (2003) 987–994.
[23] W. Yuan, R.S. Mishra, B. Carlson, R.K. Mishra, R. Verma, R. Kubic, Scripta Mater. 64 (2011) 580–583.
[24] Y.S. Sato, H. Kokawa, K. Ikeda, M. Enomoto, S. Jogan, T. Hashimoto, Metall. Mater. Trans. A 32A (2001) 941–948.
[25] U. Suhuddin, S. Mironov, Y.S. Sato, H. Kokawa, C.W. Lee, Acta Mater. 57 (2009) 5406–5418.
[26] W. Woo, H. Choo, D.W. Brown, P.K. Liaw, Z. Feng, Scripta Mater. 54 (2006) 1859–1864.
[27] J. Koike, Metall. Mater. Trans. A 36A (2005) 1689–1696.
[28] S.B. Yi, C.H.J. Davies, H.G. Brokmeier, R.E. Bolmaro, K.U. Kainer, J. Homeyer, Acta Mater. 54 (2006) 549–562.
[29] M.R. Barnett, Z. Keshavarz, A.G. Beer, D. Atwell, Acta Mater. 52 (2004) 5093–5103.
[30] F. Kaiser, D. Letzig, J. Bohlen, A. Styczynski, C. Hartig, K.U. Kainer, Mater. Sci. Forum 419–422 (2003) 315–320.
[31] R.B. Figueiredo, T.G. Langdon, Mater. Sci. Eng. A 430 (2006) 151–156.
[32] O.A. Kaibyshev, I.V. Kazachkov, R.M. Galeev, J. Mater. Sci. 16 (1981) 2501–2506.
[33] J.A.d. Valle, M.T. Pérez-Prado, O.A. Ruano, Metall. Mater. Trans. A 36A (2005) 1427–1438.
[34] S.R. Agnew, M.H. Yoo, C.N. Tomé, Acta Mater. 49 (2001) 4277–4289.
[35] S.R. Agnew, O. Duygulu, Int. J. Plasticity 21 (2005) 1161–1193.
[36] M.H. Yoo, Metal. Trans. A 12A (1981) 409–418.
[37] H. Watanabe, M. Fukusumi, H. Somekawa, T. Mukai, Mater. Sci. Eng. A 527 (2010) 6350–6358.